NORSAR ROYAL NORWEGIAN COUNCIL FOR SCIENTIFIC AND INDUSTRIAL RESEARCH

Scientific Report No. 3-76/77

FINAL TECHNICAL SUMMARY

1 April - 30 September 1977

Edited by

H. Gjøystdal

Kjeller, 31 October 1977

Sponsored by
Advanced Research Projects Agency
ARPA Order No. 2551

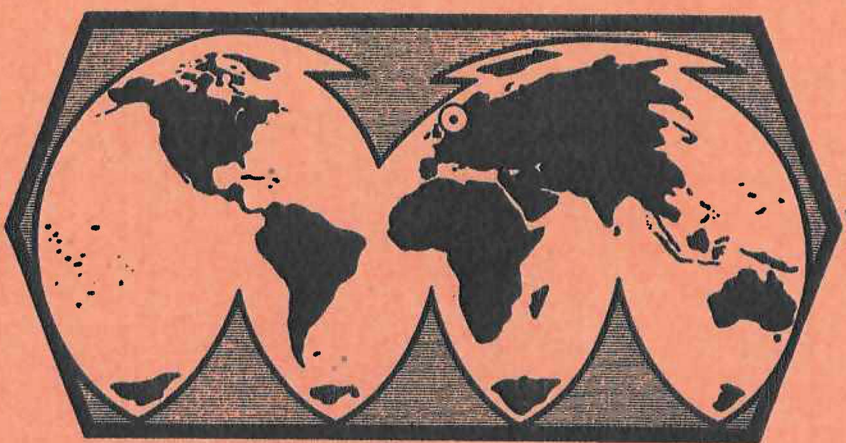

VI.3 P-wave Amplitude Observations Across NORSAR - Observational and Theoretical Results

The variability in short period P-wave amplitude observations has intrigued seismologists for many years as manifested through the numerous magnitude scales proposed and amplitude-distance tables published. Better sampling of this kind of phenomenon as offered by the large aperture seismic arrays clearly indicates that the mentioned amplitude variability is more severe than generally assumed. For example, amplitude variations amounting to one magnitude unit are often observed across the NORSAR array. Furthermore, the amplitude distribution is approximately lognormal as demonstrated by Ringdal et al (1975). Intuitively, the reported amplitude anomalies must have a counterpart in structural heterogeneities in the array siting area, and this is the problem addressed in this study.

Recently Aki et al (1977) have developed a flexible block modelling procedure for estimating deterministically the 3-D seismic velocity anomaly structure beneath large aperture arrays and similar types of seismograph networks using travel time observations. To our knowledge, no similar study has been undertaken to interpret extensive P-wave amplitude anomalies. This is perhaps not surprising as at least the NORSAR-reported amplitude anomalies often vary very rapidly with changing epicentral distance and azimuth in contrast to the relatively slowly varying time anomalies. Some of the basic assumptions underlying our approach to tackle the amplitude problem are as follows (reference array is NORSAR):

- In the context of P time and amplitude anomalies, the postulated inhomogeneous layer can be treated as an equivalent thin lens located at the depth D.
- The scales of the anomalies are such that ray theory is applicable.

The wave equation in analysis of time-derived lens models

Assuming slowly varying physical properties, the acoustic wave equation is applicable (for details, see Claerbout, 1976):

$$p_{xx} + p_{yy} + p_{zz} - c^2 p_{tt} = 0 \quad (1)$$

where p denotes pressure variations in the medium, c is velocity and the subscripts denote partial derivatives. For c = constant a solution of (1) corresponding to a plane harmonic wave travelling in the z direction is

$$p' = p_0 e^{i(mz-\omega t)} \quad (2)$$

where $m = \omega^2 c^2$ is the wavenumber and p_0 = constant.

Now, a solution of (1) may be sought which has the form (2) but with p_0 now a slowly varying function of position in the medium. Substituting (2) into (1) and dropping the zero subscript then gives

$$p_{xx} + p_{yy} + p_{zz} + 2imp_z - m^2 p + p\omega^2/c^2 = 0 \quad (3)$$

If the ray deflections are small, the pressure (or equivalent amplitude) modulation p will be slow and the term p_{zz} will be relatively small. Ignoring the latter term, we get:

$$p_z = \frac{1}{2\pi} (p_{xx} + p_{yy} + \varepsilon m^2 p) \quad (4)$$

where $\varepsilon = (\omega^2/m^2c^2 - 1)$ and $c = c(x,y,z)$.

Equation (4) is easily solved using finite difference methods. The boundary conditions to be applied on the artificial grid boundaries are somewhat arbitrary and are here chosen as zero slope.

Calculation of time delays from amplitudes for a thin lens

Consider a plane wave with uniform amplitude p_0 moving vertically upwards and passing through the horizontal thin lens L in the plane z = 0. The wavefront advances in the direction of the rays which in the vicinity of each point on the wavefront converge or diverge. Let ρ_1, ρ_2 denote the two principal radii of curvature at point p(x,y,z) on the wavefront and let ξ, η be local cartesian coordinates in the z-plane corresponding to the principal planes of curvature at P. From ray theory we have that the energy flux through the area ABCD and EFGH (see Fig. VI.3.1) are equal, thus

$$p^2/p_0{}^2 = (\text{AREA})_{\text{ABCD}}/(\text{AREA})_{\text{EFGH}} = \frac{\rho_1+R}{\rho_1} \cdot \frac{\rho_2+R}{\rho_2} \tag{5}$$

where R is the mean distance fromthe lens. The principal radii of curvature are given by

$$1/\rho_1 = r_{\xi\xi} \quad ; \quad 1/\rho_2 = r_{\eta\eta} \tag{6}$$

where r is the advance of the wavefront from the lens. Substituting into (5) gives

$$r_{\xi\xi} + r_{\eta\eta} + Rr_{\xi\xi}r_{\eta\eta} = (p^2/p_0{}^2-1)/R \tag{7}$$

Transforming to cartesian coordinates:

$$r_{xx} + r_{yy} + R\{r_{xx}r_{yy}-(r_{xy})^2\} = (p^2/p_0{}^2-1)/R \tag{8}$$

This differential equation, together with suitable boundary conditions, determines the shape of the wavefront in terms of the relative amplitudes at distance R from the lens. If $|\frac{R}{\rho_1}|$ and $|\frac{R}{\rho_2}|$ are small the nonlinear terms may be neglected. The equation then becomes Poisson's equation which has a unique solution within a given region if r is specified on its boundary. If $|\frac{R}{\rho_1}|$ and $|\frac{R}{\rho_2}|$ are moderate, the nonlinear terms may be transferred to the right-hand side of the equation and treated as perturbation terms. The nonlinear equation can then be solved using standard techniques.

Derivation of thin lens models

Projection of travel time data.

The travel time data we have used consist of relative arrival times at each of NORSAR's 22 subarrays for about 180 seismic event locations in the distance range 25^o-135^o. This set includes those of Berteussen (1974) together with an additional 90 events to obtain an improved coverage of certain azimuth sectors. If the true directions of approach of rays at surface receivers were known, the relative time delays required to be produced by the hypothetical thin lens could be obtained by projecting the observed delays back to points on the lens where corresponding rays passed through. We have used the NORSAR least squares plane wavefront direction as the ray approach direction at each subarray for each event. The relative time delays to be produced by the lens are determined by projecting the observed delays to the plane of the lens using the NORSAR direction. A thin lens model thus constructed is shown in Fig. VI.3.2a and VI.3.2b. The errors associated with the approximation are of the order of 0.1 sec.

To summarize, simple thin lens models have been constructed which can account for about 80% of the mean square observed travel time anomalies. The optimum lens depth is found to be around 150 km though depths of between 100 and 200 km satisfy the time delay data almost equally well.

Projection of amplitude data

Direct comparison of amplitude data with theoretical results for individual events is hardly warranted because of the small-scale variability of observed amplitudes and the large number of cases involved. For these reasons it is desirable to smooth the data and also reduce the number of comparisons that need to be made. For a simple lens-type structure this may be done by projecting the amplitude data (taken from Berteussen and Husebye, 1974) in essentially the same way as for the times (notice that lens models give similar surface amplitude distributions for similar arrival directions apart from the horizontal translations involved). A single theoretical amplitude distribution can therefore be used for comparison with data for a range of different arrival directions. Equivalently, the theoretical amplitude distribution may be kept fixed and the data translated. The relative data translations required to correspond to results for a thin lens are given simply by projecting the amplitude data onto the plane of the lens in precisely the same manner as for the times. It is, of course, necessary in this case to introduce appropriate amplitude scaling factors (additive constants) for each event. The results obtained (see Fig. VI.3.3) show that the method works surprisingly well for the entire range of the available data. Also for the amplitude projections the best fitting projection depths are around 150-200 km.

Comparison of amplitude projections with theoretical amplitudes for the lens models

In the context of the thin lens hypothesis, amplitude projections correspond to surface amplitudes for a wave of vertical incidence. The relationship between the amplitude and time observations may therefore be examined by comparing amplitude projections with theoretical ones for models derived from the time data. For example, comparison of Figs. VI.3.3 and VI.3.4 shows that while there are discrepancies in detail, the major features of the theoretical amplitude distribution are in good agreement with those observed, in that regions of relatively high and low amplitudes occur in similar locations in each figure. A major cause of the discrepancies of small wavelength features is that amplitudes depend essentially on the curvature of the wavefront induced by the lens, and quite small errors in the inferred time delays can result in large local disturbances in the associated amplitude pattern.

Lens models derived using amplitudes

With the same assumptions as in the previous section, amplitude projections may be interpreted as representing wave amplitudes for a vertically incident wave over an extensive area of the earth's surface. In this section we treat the amplitude projections in this way and apply Eq. (8) to derive corresponding lens models to fit these amplitude projections exactly. The difference between calculated and observed lens models is shown in Fig. VI.3.5, and the differences are indeed small except for a minor area in the northeast quadrant (the correlation between these two surfaces is 0.91!)

Discussion and conclusions

The results given above clearly demonstrate that medium-scale travel time and amplitude anomalies observed at NORSAR are strongly correlated. The physical structure responsible for both may be modelled by a single homogeneous layer at a mean depth of about 200 km beneath the array. We consider, for example, that our results on amplitudes provide strong support for the hypothesis that the main travel time anomalies observed at NORSAR result almost entirely from 3-D structure which may be represented to a good first approximation as a 2-D 'layer' in the upper mantle or bottom of the lithosphere beneath the array.

In conclusion we remark that our lens models entail typical ray deflections of order 5^{o} for each one-way transit through the upper mantle so that waves reflected from the earth's surface in the vicinity of NORSAR would be effectively scattered in a range of about $\pm 10^{o}$ from the mean ray direction. Such scattering is consistent with similar scattering effects in other regions of the upper mantle as indicated by observations and interpretation of the seismic phases PP and P'P' (see, e.g., King et al, 1975; Haddon et al, 1977). The results presented above demonstrate very clearly the inherent problems in properly estimating m_b-magnitudes.

R.A.W. Haddon, Univ. of Sydney
E.S. Husebye

References

Aki, K., A. Christoffersson and E.S. Husebye (1977): Determination of the three-dimensional seismic structure of the lithosphere, J. Geophy. Res., 82, 277-296.

Berteussen, K.-A. (1974): NORSAR location calibrations and time delay corrections, Sci. Rep. 2-73/74, NTNF/NORSAR, Kjeller, Norway.

Berteussen, K.-A. (1977): Moho depth determinations based on spectral ratio analysis of NORSAR long period P-waves, Phys. Earth Planet. Inter., 15, 13-27.

Berteussen, K.-A., and E.S. Husebye (1974): Amplitude pattern effects on NORSAR P-wave detectability, Sci. Rep. 1-74/75, NTNF/NORSAR, Kjeller, Norway.

Claerbout, J.F. (1976): Fundamentals of Geophysical Data Processing, McGraw-Hill, New York.

Haddon, R.A.W., and E.S. Husebye (1977): Joint interpretation of P-wave time and amplitude anomalies in terms of 2-D lithospheric heterogeneities, manuscript in preparation.

Haddon, R.A.W., E.S. Husebye and D.W. King (1977): Origins of precursors to P'P', Phys. Earth Planet. Inter., 14, 41-71, 1977.

King, D.W., E.S. Husebye and R.A.W. Haddon (1975): Precursors to PP, Phys. Earth Planet. Inter., 10, 102-127.

Ringdal, F., E.S. Husebye and A. Dahle (1975): P-wave envelope representation in event detection using array data, Proceedings, NATO Advanced Study Institute 'Exploitation of Seismograph Networks' (K.G. Beauchamp, ed.), Nordhoff-Leiden, 353-372.

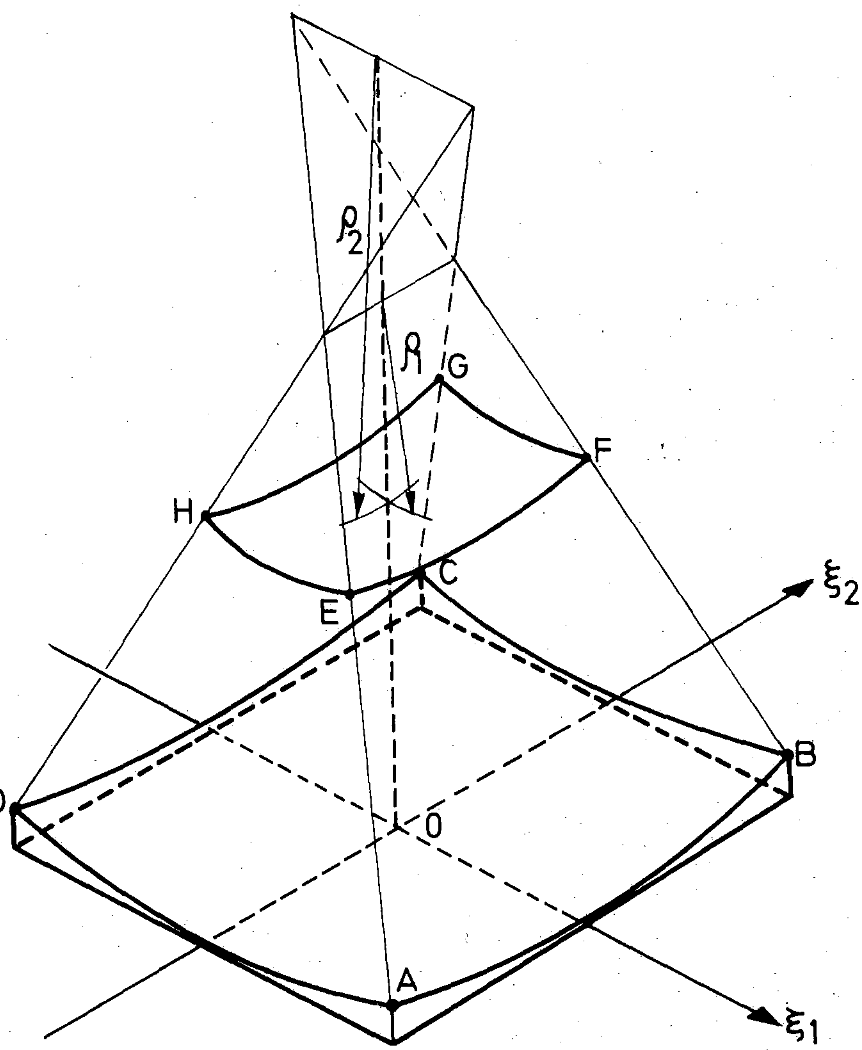

Fig. VI.3.1 Schematic illustration of focusing effect for a perturbed wavefront. The energy flux through the areas ABCD and EFGH is the same. The principal radii of curvature of the wavefront in the latter area are ρ_1 and ρ_2. The rays in the vicinity of each point of the wavefront converge or diverge to or from the two centers of curvature as shown in the figure.

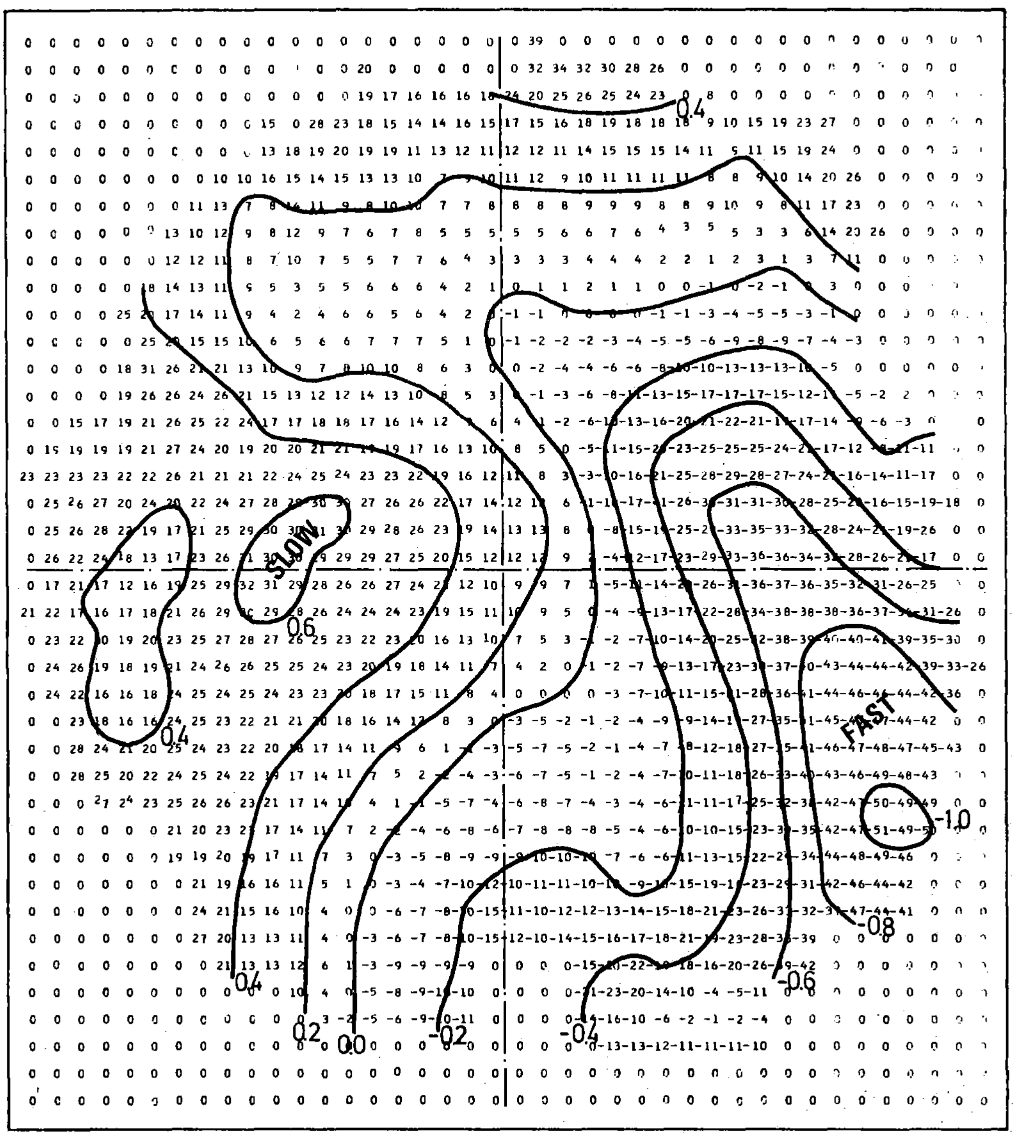

Fig. VI.3.2a Thin lens model for a depth of 150 km constructed by projecting and averaging travel time residuals as described in the text. The area shown is a 400 km x 400 km square whose center is located vertically below the center of the array. The numbers at each 10 km x 10 km grid point represent time delays produced by the lens at the point. For computer printing convenience the time values are in units of 0.02 sec, while the contouring intervals are unscaled. Note the systematic trend in time delays from positive on the left to negative on the right of the figure.

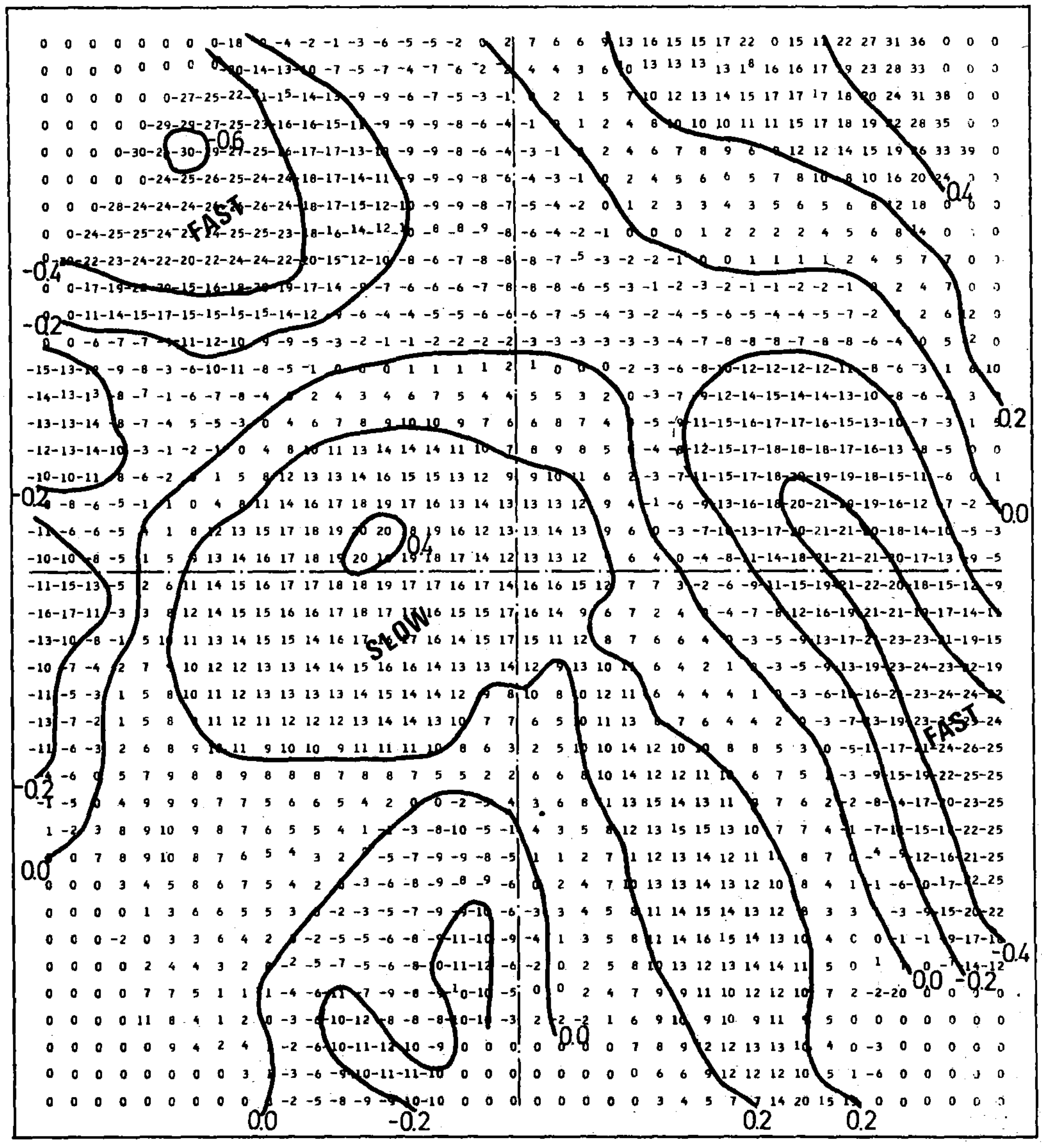

Fig. VI.3.2b Thin lens model for a depth of 200 km in which the systematic trend evident in Fig. VI.3.2a has been removed as described in the text. Other details as in caption for Fig. VI.3.2a.

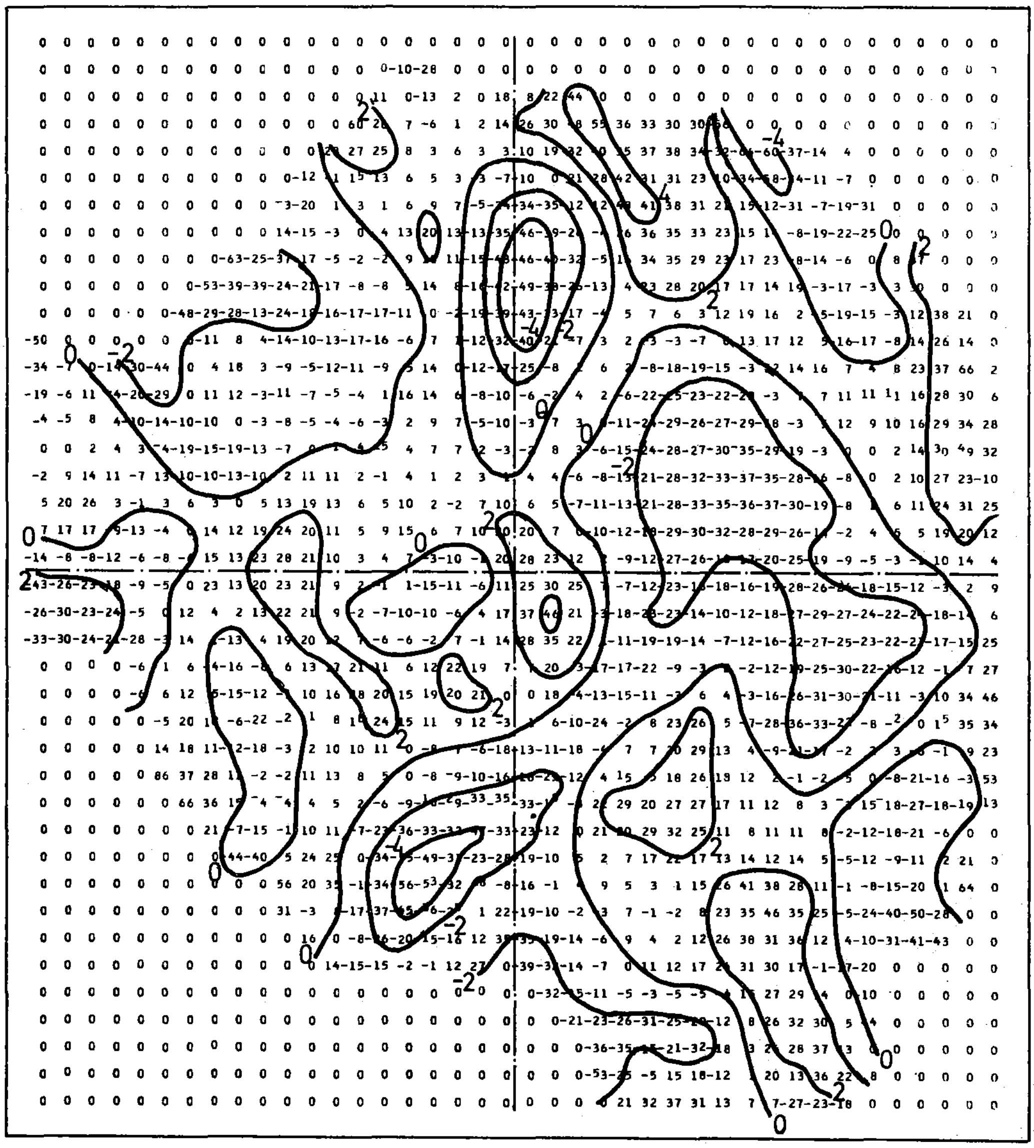

Fig. VI.3.3 Amplitude projection for D=200 km using the projection procedure described in the text. The numbers give amplitude values in dB multiplied by 10, while the contours are in non-scaled dB-units. Note the extensive regions of relatively high and low amplitudes.

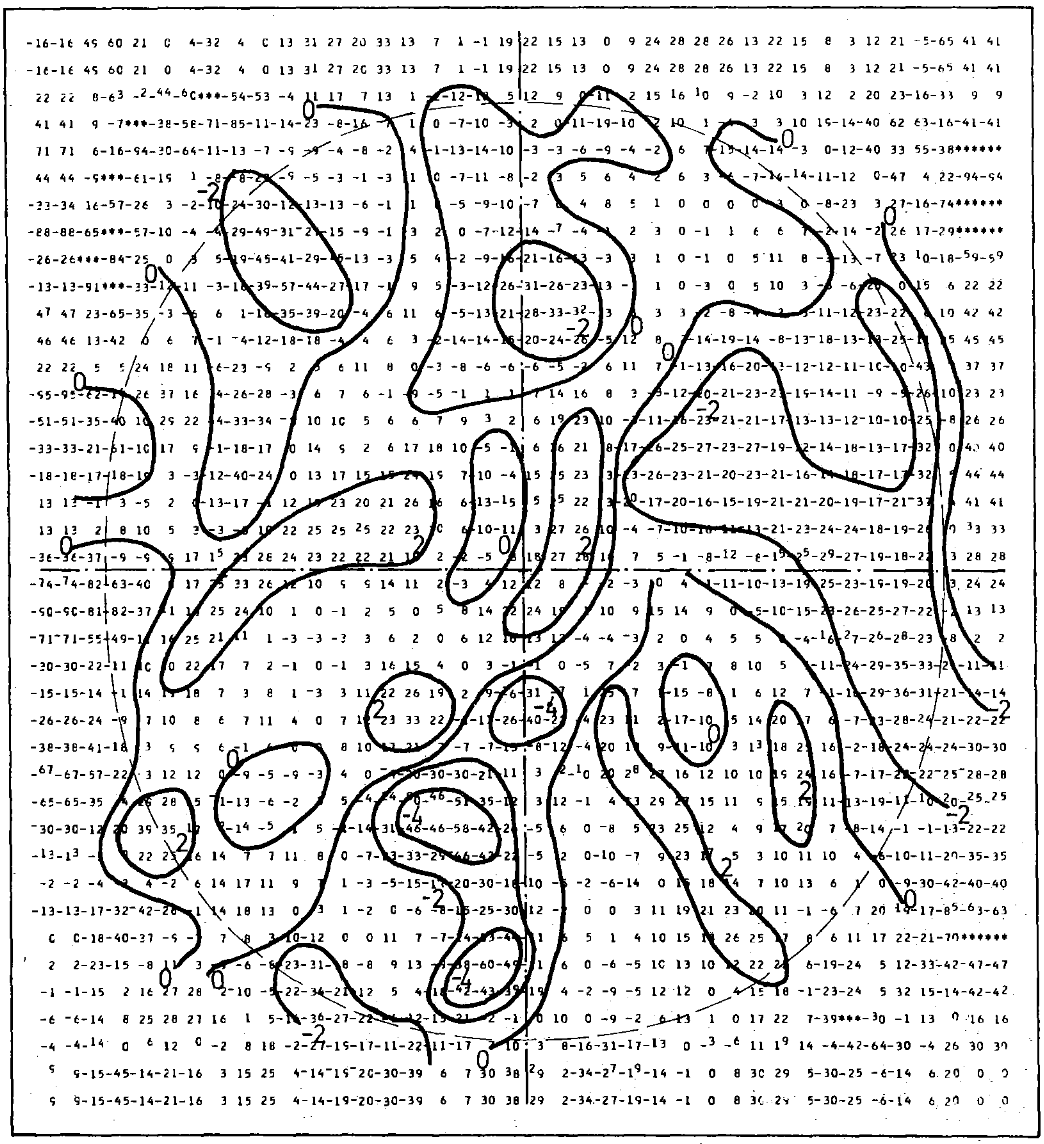

Fig. VI.3.4 Theoretical amplitudes for a wave of vertical incidence for the thin lens model shown in Fig. VI.3.2b. The amplitude values are in units of dB multiplied by 10, while the contours shown are in non-scaled dB-units. Note that the area outside the dashed circle in the figure should be disregarded because of spurious effects associated with the boundaries of the lens. Positive and negative values indicate relatively large and small amplitudes, respectively.

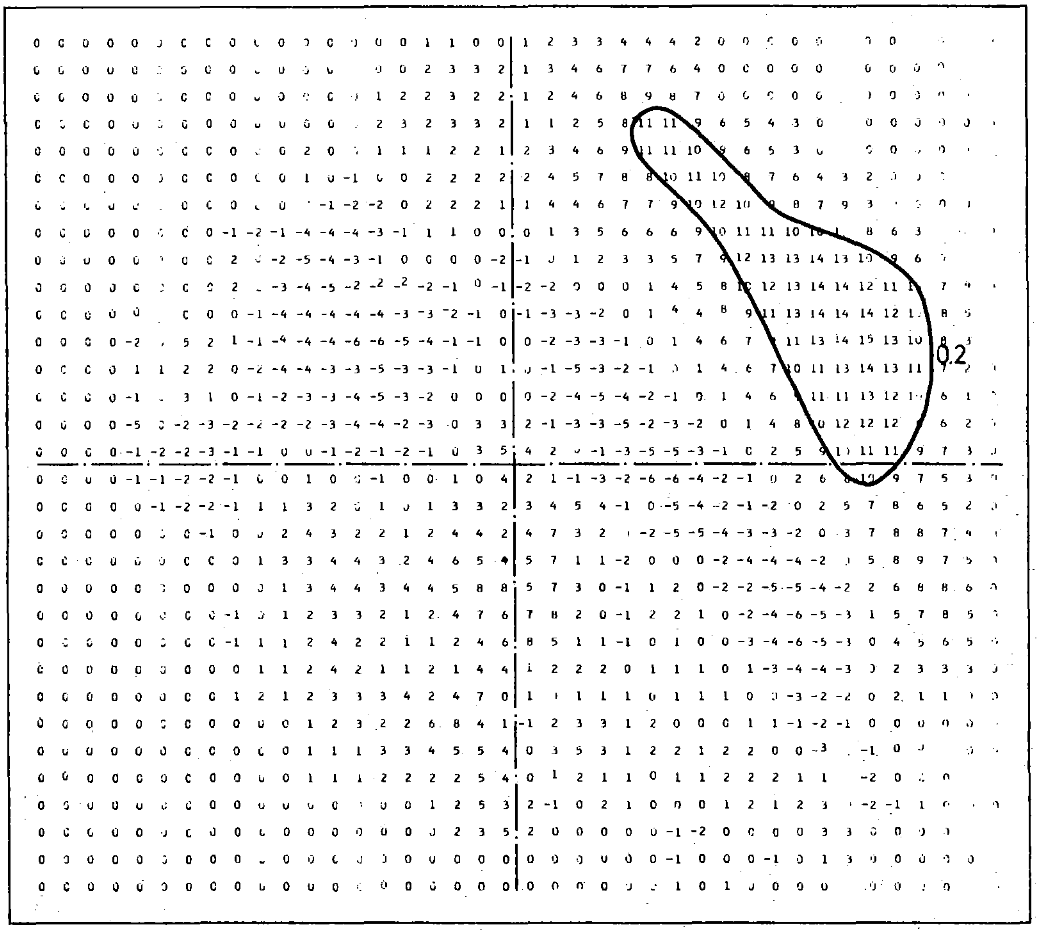

Fig. VI.3.5 Differences between corresponding grid point time delays for the lens models shown in Figs. VI.3.2b and those derived from Fig. VI.3.3. Note that with the exception of the northeast quadrant, the differences are small. This result implies that the travel time and amplitude anomalies may be jointly satisfied by a suitable thin lens model.